

## PLASTIC DEFORMATION OF MAGNESIUM ALLOY SUBJECTED TO COMPRESSION-FIRST CYCLIC LOADING

Soo Yeol Lee<sup>1,2</sup>, Michael A. Gharghoury<sup>2</sup>, and John H. Root<sup>2</sup>

<sup>1</sup> Department of Materials Engineering, The University of British Columbia, Vancouver, B.C. V6T 1Z4, Canada

<sup>2</sup> Canadian Neutron Beam Centre, National Research Council Canada, Chalk River, ON K0J 1J0, Canada

Keywords: Magnesium, Plastic deformation, Twinning, Neutron diffraction

### Abstract

In-situ neutron diffraction has been employed to study the deformation mechanisms in a precipitation-hardened and extruded Mg-8.5wt.% Al alloy subjected to compression followed by reverse tension. The starting texture is such that the basal poles of most grains are oriented normal to the extrusion axis and a small portion of grains are oriented with the basal pole parallel to the extrusion axis. Diffraction peak intensities for several grain orientations monitored in-situ during deformation show that deformation twinning plays an important role in the elastic-plastic transition and subsequent plastic deformation behavior. Significant non-linear behavior is observed during unloading after compression and appears to be due to detwinning. This effect is much stronger after compressive loading than after tensile loading.

### Introduction

Magnesium and its alloy are currently the subject of many studies due to their potential use for lightweight structures in the automotive and aircraft industries, and for portable electronic devices [1,2]. The poor room-temperature formability of these alloys arises from the limited number of available slip systems [3,4]. The primary slip system in magnesium is  $\langle a \rangle$  slip with a  $1/3\langle 11\bar{2}0 \rangle$  Burgers vector on the close-packed (0002) basal plane. Non-basal  $\langle a \rangle$  slip on the  $\{10\bar{1}0\}$  prismatic and  $\{10\bar{1}1\}$  pyramidal planes has also been observed. None of these slip modes provide deformation along the c-axis. Deformation twinning can provide deformation along the c-axis;  $\{10\bar{1}2\}\langle 10\bar{1}1 \rangle$  tensile twinning is commonly observed at room temperature in favorably oriented grains, resulting in a strong tension-compression asymmetry in textured specimens due to the unidirectional nature of twinning [5-7]. Deformation twinning results in texture evolution because it gives rise to a large lattice reorientation relative to the parent grain [8-10]. Neutron diffraction has been successfully used, during deformation, to investigate bulk texture evolution due to twinning, as well as internal stress distributions among the different crystallographic orientations [11-14].

In this work, lattice strains and diffraction peak intensities for several grain orientations were measured in an extruded Mg-8.5wt.% Al alloys during deformation using neutron diffraction. The loading path consisted of compression followed by reverse tension.

### Experimental details

The binary alloy was supplied by the P echiney Research Centre, Voreppe, France. The material was solution treated and aged. The volume fraction of  $\beta$ -Mg<sub>17</sub>Al<sub>12</sub> precipitates is ~10%. The precipitates are plate shaped, with an average thickness of 165nm, a length that varies from 6 to 20 $\mu$ m and a length to width ratio between 2 and 6. The grains are equiaxed with an average size of ~60  $\mu$ m. Neutron diffraction experiments were conducted on the L3 spectrometer of the Canadian Neutron Beam Centre, Chalk River Laboratories, Canada. Data were acquired for the (10-10), (10-11) and (0002) diffraction peaks with the scattering vector parallel to and normal to the applied load. The experiments were conducted in-situ, which allowed us to observe lattice strain evolution and bulk texture development as a function of applied load. The material microstructure and neutron diffraction experiments are described in detail elsewhere [11].

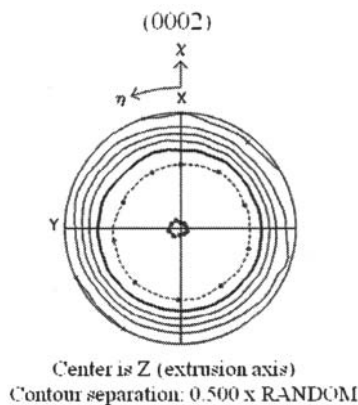


Figure 1. (0002) pole figure showing initial texture of the test material measured by neutron diffraction. The pole figure is contoured in multiples of random distribution (m.r.d) with the thick solid black line corresponding to 1 m.r.d. The contour levels above and below 1 m.r.d are shown by solid and dotted lines, respectively, in 0.5 m.r.d steps.

### Results and Discussion

The (0002) basal pole figure for the as-received material is shown in Fig. 1. The center of the pole figure corresponds to the extrusion axis. The (0002) basal planes in most grains are parallel

or close to the extrusion axis, with a correspondingly small fraction of grains with the basal planes perpendicular to the extrusion axis. Fig. 2 shows the macroscopic stress-strain response of the alloy subjected to compression followed by reverse tension. The symbols in the graph correspond to points in the loading history at which diffraction data were acquired. In compression up to  $-100$  MPa, the alloy shows mainly elastic deformation, with some limited plasticity. Beyond  $-100$  MPa, the elastic-plastic transition is well underway, though plasticity is not fully developed. During unloading after compression and reloading in tension, the stress-strain response is clearly non-linear, showing a typical s-shaped profile. The material undergoes general yielding in tension at  $\sim +125$  MPa. The unloading portion of the curve, after tensile loading, is again non-linear, but the effect is less significant than after compression.

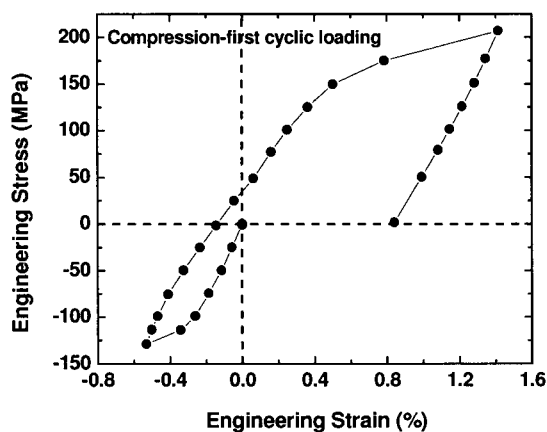


Figure 2. Macroscopic stress-strain response of the extruded Mg-8.5wt.%Al alloy. The symbols correspond to points in the loading history at which diffraction data were acquired.

The integrated intensity data acquired during loading for all measured reflections are shown in Fig. 3. For these measurements, the scattering vector was parallel to the loading direction. The data are plotted chronologically as functions of the applied load in order to show clearly how the measured values change during the test. The  $(0002)$ ,  $\{10-11\}$  and  $\{10-10\}$  orientations have the basal poles (*c*-axes) oriented at  $0^\circ$ ,  $61.9^\circ$  and  $90^\circ$ , respectively, relative to the extrusion direction (ED), which is also the loading direction. Thus, the  $\{10-10\}$  and  $(0002)$  grains are favorably oriented for extension twinning in compression and tension, respectively. Neither family of grains is oriented favorably for  $\langle a \rangle$ -slip on any plane. In contrast, the  $\{10-11\}$  grains are favorably oriented for basal  $\langle a \rangle$  slip. The  $\{411\}$  reflection is from the  $\beta$ -Mg<sub>17</sub>Al<sub>12</sub> precipitates.

During initial loading in compression, the  $(0002)$  intensity starts to increase beyond  $\sim -100$  MPa, while the  $\{10-10\}$  intensity decreases concurrently. This corresponds with the macroscopic yield point ( $\sim -100$  MPa). The intensity of a diffraction peak changes when the amount of material oriented for Bragg diffraction changes. Since the volume sampled by the neutron beam is constant, this can only occur if there is a phase change, or

if material is re-oriented. In the present case, no phase change occurs. Thus, a decrease in intensity of a given reflection means that the contributing grains have twinned – i.e. that some of the grain volume is no longer appropriately oriented for diffraction. Conversely, an increase in intensity means that a conjugate set of grains has undergone twinning, such that additional material contributes to the intensity. In the case of magnesium,  $\{10-12\}$  extension twinning results in an  $86.6^\circ$  reorientation of the crystal lattice, which would convert an  $\{10-10\}$  orientation into an  $(0002)$  orientation and vice versa.

As the load increases from  $-100$  MPa to  $-130$  MPa, the  $(0002)$  intensity increases sharply due to  $\{10-12\}\langle 10-11 \rangle$  extension twinning in grains with the *c*-axis normal to the loading direction, such as the  $\{10-10\}$  grains. It is thus likely that this extension twinning is responsible for the observed plastic deformation behavior shown in Fig. 2. Since many grains in the starting material have the *c*-axis approximately normal to the loading direction, the lattice reorientation due to extension twinning will reorient the material into the  $(0002)$  orientation. The effect on the intensity of the  $(0002)$  reflection is thus very strong, resulting in a 3-fold increase even at very low macroscopic strain.

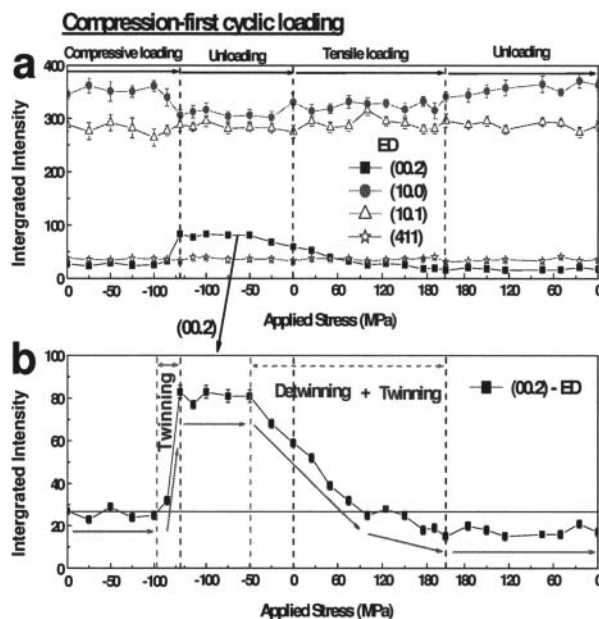


Figure 3. (a) Intensity variations as functions of applied load during the deformation shown in Figure 2; (b) Close-up of intensity variations for the  $(0002)$  reflection. Measured  $(hkl)$  plane normal is parallel to the applied loading direction, which is the same as the extrusion direction (ED).

When the sample is unloaded after compression, the intensity of the  $(0002)$  peak remains stable down to an applied stress of  $\sim -50$  MPa, and then decreases gradually. The intensity falls by about 40% during unloading to zero load, indicating that about 40% of the twinned volume has detwinned during unloading after compression. It is possible that the parent  $(0002)$  grains undergo compressive  $\{10-11\}\langle 10-12 \rangle$  twinning during unloading after

compression, but this is unlikely as this type of twinning is very uncommon, and is generally found to contribute little to lattice reorientation during deformation. This detwinning behavior is thought to contribute significantly to the non-linear behavior observed in Fig. 2.

During reverse loading in tension, detwinning continues until the (0002) intensity at the start of the test is fully recovered at about +100 MPa. As the applied load increases from 100 MPa to 205 MPa, the (0002) intensity continues to decrease, but at a lower rate. At this point, it appears that the (0002) minority grains undergo {10–12} extension twinning. During unloading after the tensile portion of the stress-strain curve, the (0002) peak intensity does not change, suggesting that the twinned material in the minority (0002) grains does not undergo significant detwinning.

### Summary

Neutron diffraction has been used to study the plastic deformation behavior of a Mg-8.5wt.%Al alloy subjected to compression followed by reverse tension. It was found that the onset of extension twinning corresponds well with the macroscopic elastic-plastic transition. The non-linear behavior during unloading after compression was more significant than that after tension. Diffraction results show that about 40% of the twinned volume detwins during unloading after compression, but that no significant detwinning occurs during unloading after tension.

### Acknowledgements

This work was supported by funding from the NSERC Magnesium Strategic Research Network. More information on the Network can be found at [www.MagNET.ubc.ca](http://www.MagNET.ubc.ca).

### References

1. M.M. Avedesian and H. Baker, *Magnesium and Magnesium Alloys*, ASM Specialty Handbook, ASM International, Materials Park, OH, 1999.
2. C. Wang, P. Han, L. Zhang, C. Zhang, X. Yan, B. Xu, J. All. Comp. 482 (2009) 540-543.
3. C.S. Roberts, *Magnesium and its Alloys*, John Wiley & Sons, Inc., New York, 1960.
4. O. Muránsky, D.G. Carr, M.R. Barnett, E.C. Oliver, P. Šittner, *Mater. Sci. Eng. A* 496 (2008) 14-24
5. P.G. Partridge, *Metall. Rev.* 12 (1967) 169-194.
6. S.R. Agnew, C.N. Tomé, D.W. Brown, T.M. Holden, S.C. Vogel, *Scripta mater.* 48 (2003) 1003-1008.
7. J. Jain, W.J. Poole, C.W. Sinclair, M.A. Gharghoury, *Scripta mater.* 62 (2010) 301-304.
8. B. Clausen, C.N. Tomé, D.W. Brown, S.R. Agnew, *Acta mater.* 56 (2008) 2456-2468.
9. G. Proust, C.N. Tomé, A. Jain, S.R. Agnew, *Int. J. Plasticity* 25 (2009) 861-880.
10. O. Muránsky, M.R. Barnett, V. Luzin, S. Vogel, *Mater. Sci. Eng. A* 527 (2010) 1383-1394.
11. M.A. Gharghoury, G.C. Weatherly, J.D. Embury, J. Root, *Phil. Mag. A* 79 (1999) 1671-1695.
12. D.W. Brown, S.R. Agnew, M.A.M. Bourke, T.M. Holden, S.C. Vogel, C.N. Tome, *Mater. Sci. Eng. A* 399 (2005) 1-12.
13. L. Wu, S.R. Agnew, D.W. Brown, G.M. Stoica, B. Clausen, A. Jain, D.E. Fielden, P.K. Liaw, *Acta mater.* 56 (2008) 3699-3707.
14. O. Muránsky, M.R. Barnett, D.G. Carr, S.C. Vogel, E.C. Oliver, *Acta mater.* 58 (2010) 1503-1517.